Deep Mining 2024 – P Andrieux & D Cumming-Potvin (eds)

doi:10.36487/ACG_repo/2465_59

Stress inversion from slip-type and crush-type seismic events in mines

Dmitriy Malovichko [a,*], **Alex Rigby** [a]

[a] *Institute of Mine Seismology, Australia*

Abstract

In the context of crustal seismology, a number of methods have been proposed for inferring stress state information from seismic data (moment tensors). These methods rely on assumptions that are often violated by mining-induced seismicity. For example, they require that sources are purely slip-type, whereas crush-type sources (failure near/around excavations and convergence of the surrounding rock mass) are frequently observed in mines. The conventional methods also cannot be applied to source mechanisms controlled by a small number of predominant faults. This paper presents a new stress inversion method (called stress inversion from mine seismicity – SIMS) that makes it possible to involve more data compared to the conventional methods; specifically crush-type seismic events associated with tunnels and slip-type events attributed to known geological structures. The performance of method is demonstrated using a synthetic case study and also data from a real mine.

Keywords: *direction of principal stresses, ratio of stress magnitudes, seismic source mechanism, dynamic stress fracturing around tunnels*

1 Introduction

Historically, earthquake mechanisms have been considered as a source of information about stress acting in the hypocentral areas. The established naming of principal axes of seismic moment tensors reflects the expected loading conditions (P-axis – pressure, T-axis – tension) and, in some early seismological analyses, these axes were interpreted as principal stress axes. However, McKenzie (1969) showed that the only restriction on the direction of maximum compressive stress, σ_1, is that it must be within the dilatational quadrant of the focal sphere. Therefore, the P-axis can be used only as a proxy of σ_1. Correspondingly, the T-axis is often considered as a proxy of minimum principal stress, σ_3.

Although a single source mechanism does not provide a strong constraint on the stress field, a set of focal mechanisms associated with randomly oriented weaknesses can be used to assess the directions of principal stresses (σ_1, σ_2 and σ_3) and the ratio of their magnitudes, which can be described by the parameter $R = (|\sigma_1| - |\sigma_2|)/(|\sigma_1| - |\sigma_3|)$. Many procedures of such assessment (often called stress inversion) have been proposed, starting from the pioneering works of Angelier (1984), Gephart & Forsyth (1984), Michael (1984, 1987) and Harmsen & Rogers (1986). Typically they rest on the following assumptions:

- The stress field is homogeneous within the area of analysis.
- Source mechanisms correspond to a double-couple model.
- Actual and potential slip planes are randomly oriented, i.e. earthquakes are not controlled by a small number of predominant structures.
- The direction of slip is co-oriented with the direction of shear traction on the slip surface.

* Corresponding author. Email address: Dmitriy.Malovichko@IMSI.org

Provided that the above assumptions are met, stress inversion methods developed for tectonic earthquakes can be employed for seismicity recorded on a smaller scale. The results of applying existing stress inversion methods to seismic data recorded in mines were discussed by Urbancic et al. (1993), Trifu & Shumila (2011), Brzovic et al. (2017), Abolfazlzadeh & McKinnon (2017) and Malovichko (2022).

However it is important to note that meeting these assumptions in a mining context typically requires excluding a significant portion of the seismic catalogue. For example, non-double-couple mechanisms that are often observed in mines need to be filtered out. Furthermore, seismic events with double-couple mechanisms corresponding to known geological structures (e.g. faults and thin dykes) also need to be excluded from the inversion. It is of practical value to include the aforementioned data in stress inversion. This constitutes the principal objective of the paper.

A method of stress inversion that takes the specifics of seismic data recorded in mines into account is proposed in Section 2. The method's performance is demonstrated in Section 3 using a synthetic catalogue of mining-induced seismic events modelled for several stress field variants. Application of the method to data from a real mine is presented in Section 4. The method's limitations and potential future improvements are discussed in the last section.

2 Method

Similar to conventional stress inversion methods, the proposed approach requires the selection of seismic data from a spatio-temporal domain within which the stress field can be considered as homogeneous, i.e. a single stress tensor has to agree with the source mechanisms of the selected event set. It is important to keep in mind the scale of the assumed homogeneity. For typical configurations of mine-wide seismic monitoring systems (sensor spacing in the order of hundreds of metres), source mechanisms are calculated using seismic signals with the wavelengths in the order of tens or hundreds of metres. Therefore they characterise the inelastic deformation and driving stress within the rock mass volumes of similar dimensions. At such a scale the mechanisms cannot describe stress heterogeneities attributed to volumes with sub-metre or few-metre dimensions (e.g. concentration of stresses on the sides of tunnels or isolated stopes). The seismic data discussed below is relevant for mine-wide monitoring environments and the scale of inverted stress corresponds to tens and hundreds of metres.

Many seismic events recorded in mines have double-couple mechanisms and can be interpreted as episodes of sudden slip along an existing weaknesses (shown as F1–F3 in Figure 1) or shear rupture of the intact rock mass (shown as S1–S4 in Figure 1). In the former case, one of the nodal planes of the mechanism matches the weakness surface in terms of orientation. The event can be located away from the weakness (e.g. case F1 in Figure 1), however, this may be due to source-location uncertainty. The event can still be associated with the considered weakness provided that the distance to the weakness is less than the expected location error. The direction of slip for the nodal plane matching the weakness surface has to correlate with the direction of shear traction resolved for the weakness. Therefore the angle between these two directions (spanning 0 to 180°) quantifies the misfit between the source mechanism and stress state.

Scattered seismicity (S1–S4 in Figure 1) can be utilised in the inversion in a similar way as in the classic focal mechanism stress inversion (FMSI) method (Gephart 1990; Hardebeck & Hauksson 2001). In particular, the shear traction is resolved for both nodal planes and compared with the corresponding slip direction. The smaller of these two angular differences (ranging between 0 and 180°) is considered as the misfit[1].

Events with non-double-couple source mechanisms are frequently observed in mines. For example, crush-type events (Ryder 1988) have a significant negative isotropic (implosive) component and

[1] The conventional FMSI method utilises the minimum angle of rotation of the focal mechanism about any axis, however, this paper uses the simpler metric, allowing the rotation of mechanisms only about the poles/normals of nodal planes.

'pancake-shape' deviatoric component. If such events are attributed to tunnels they can be interpreted as episodes of sudden stress fracturing (increase in the depth of damage) and associated convergence of the surrounding rock mass (Malovichko 2020; Malovichko & Rigby 2022). The direction of convergence is controlled by the maximum principal stress within the plane orthogonal to the tunnel's axis. Given that the P-axis of a source describes the direction of convergence, the angular difference between the P-axis and maximum in-plane stress quantifies the misfit (spanning 0 to 90°) between the seismic data and stress state. Figure 1 illustrates the relation between crush-type mechanisms and stress fracturing around tunnels. The events are expected to be co-located with tunnels (e.g. cases C1 and C2), however, the error of seismic location may result in plotting the sources away from the tunnels (e.g. case C3), so this needs to be taken into account when selecting the data.

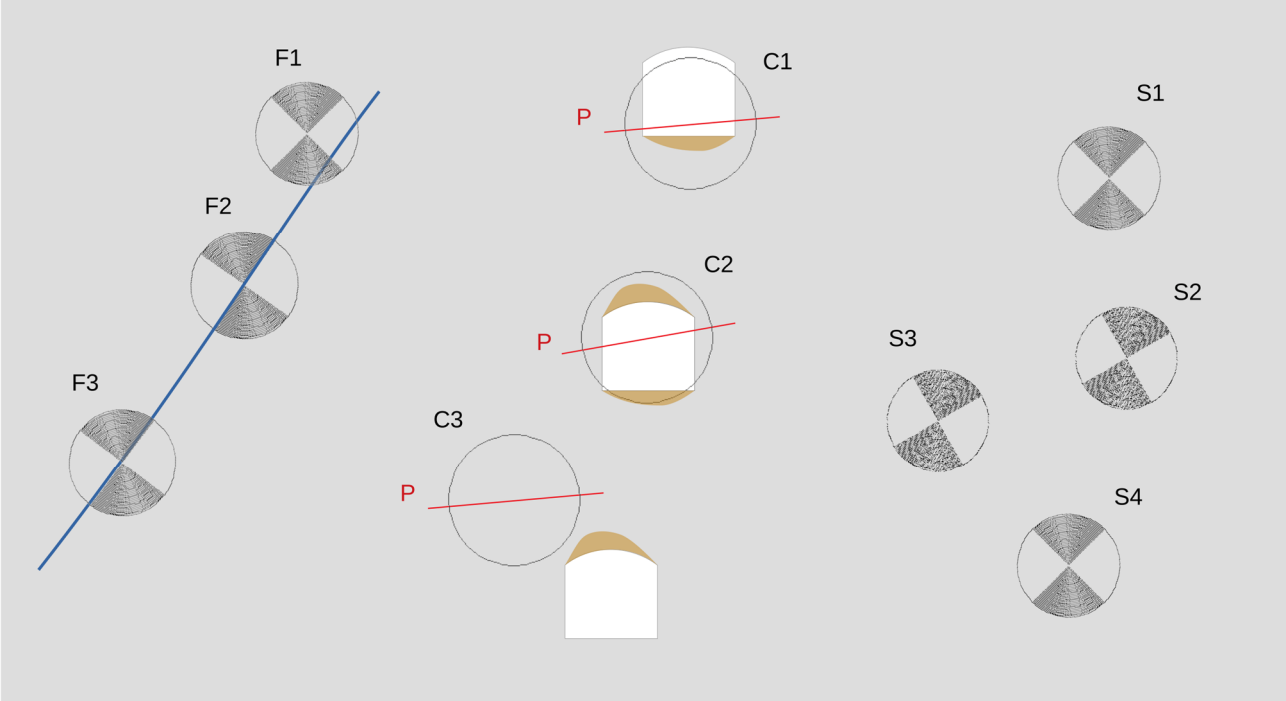

Figure 1 **Schematic representation of seismic data used in the proposed stress inversion method. Events F1–F3 with double-couple mechanisms are associated with a known fault (shown in blue). Events C1–C3 have crush-type mechanisms and spatially correlate with tunnels. These can be interpreted as episodes of sudden stress fracturing in the back and/or floor of the tunnels (shown in brown) and associated convergence of the surrounding rock mass. Events S1–S4 have double-couple mechanisms and do not have clear relation to a particular geological structure. All the plotted events are considered to be far from large-scale excavations (e.g. stopes, caves) and the stress field within the shown region can be assumed to be homogeneous**

The types of events and measures of misfit between the mechanisms and stress state discussed are summarised in Table 1.

Table 1 Description of classification of seismic data and corresponding misfits adopted in the proposed stress inversion method

Event type	Classification rule	Misfit
Slip-type events associated with known geological structures	Slip-type source mechanism Distance between the source and structure is less than FX m One of the nodal plane poles is within FY° from the normal to the nearest face of structure surface Distance between the source and large-scale excavations (e.g stopes and caves) is more than FZ m	Angle between the slip direction for the nodal plane matching the structure and the shear traction direction resolved for the nearest face of the structure surface Ranges from 0 to 180°
Crush-type events associated with tunnels	Crush-type source mechanism Distance between the source and an active (existing at the time of the event) tunnel is less than CX m	Angle between the P-axis of the mechanism and the maximum principal stress within plane orthogonal to the tunnel axis Ranges from 0 to 90°
Scattered slip-type events	Slip-type source mechanism Event does not belong to the above classes Distance between the source and large-scale excavations (e.g. stopes and caves) is more than SX m	Smallest angle between the slip direction for a nodal plane and the shear traction direction resolved for the same nodal plane Ranges from 0 to 180°

The proposed inversion of stress state, SIMS, is implemented using the following computational procedure:

- Seismic data recorded at a mine is classified according to the rules listed in Table 1. The classification requires: a structural model (specifically, wireframes of thin geological structures prone to slip), wireframes of large-scale excavations (i.e. caves and stopes) that can significantly disturb the stress at the scale of interest, and centrelines of active tunnels (existing at the time of the selected seismic events). The output of this step is three sets of events with mechanisms: FN fault-related events, CN tunnel-related events and SN scattered events. Any one or two of these sets can be empty (i.e. up to two of FN, CN or SN can be zero).
- Stress states are generated by the random rotation of principal axes following the procedure described by Kagan (1991) and random selection of the parameter R. Note that the magnitudes of principal stresses are involved in the inversion only in terms of their contribution to R. Therefore the magnitudes of isotropic and deviatoric components of stress tensor do not affect the results. The conventional stress inversion methods used for tectonic earthquakes have the same limitation. The total number of random stress states has to be of the order of tens of thousands (25,000 was used in the examples presented in the next sections).
- For each stress state, the misfit angle is calculated for every event in every dataset. The average misfit is computed for each event set as well as for the combined dataset (including all three event sets). The averaging for the combined dataset involves weighting of the constituent misfits. This is needed to take differences in misfit ranges into account (from 0 to 180° for fault-related and scattered events and from 0 to 90° for tunnel-related events) and to balance the amounts of contributing event types (i.e. to reduce the effect of a particular event type that is disproportionately represented compared to other types). The results discussed in the next sections adopt a weighting factor of 1 for structure-related and scattered events, and 0.25 for tunnel-related events.

- The selected percentage, PCT, of stress states with the smallest misfit are averaged and considered as an inverted solution. This is done for misfits of each event type as well as for the total misfit based on the combined dataset. PCT = 5% is used in the cases presented in the next two sections.
- The PCT percentile misfit is plotted on the stereonets of principal stress directions ($\sigma_1, \sigma_2, \sigma_3$). The histogram of R shows all stress samples (not just those with misfit below PCT). These plots serve to qualitatively characterise the uncertainty of the inverted solution.

3 Application to synthetic data

The described computational procedure was tested using synthetic seismic data for a fictitious mine shown in Figure 2. The narrow-vein orebody is dipping steeply to the east (dip/dip direction = 60°/90°). A decline is located in the footwall on the southern part of the orebody. Two faults with undulated surfaces are included in the model: fault A in the hanging wall (dip/dip direction = 47°/86°) and fault B in the footwall (dip/dip direction = 47°/97°). Fault B intersects the decline. In addition, two dykes intersecting the orebody are considered: stiff and soft (i.e. high and low elastic modulus, respectively). To generate the synthetic seismic data, inelastic stress models were solved for 10 quarterly mining steps using the material point method (Nairn 2003; Basson et al. 2021). Seismicity (including crush-type events) was modelled using the clustering procedure described by Rigby (2022), which is based on that of Basson et al. (2021).

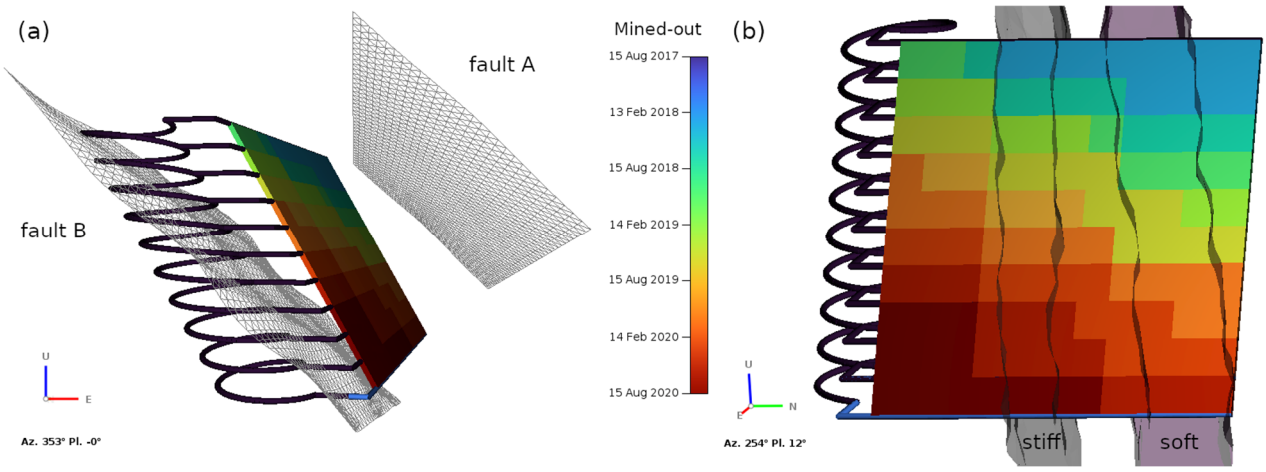

Figure 2 Mining layout for the synthetic example. The stopes are coloured according to the time of extraction done in quarterly steps. Also shown are rock mass heterogeneities: (a) faults in the hanging wall and footwall; (b) stiff and soft units intersecting the orebody

The seven stress states listed in Table 2 were considered. State A constitutes a reference state, whereas the others are variations of it:

- States B and C are obtained from state A by subsequent 60° anticlockwise rotations of σ_1 about vertical σ_3.
- States D and E vary the magnitude of σ_2.
- States F and G vary the inclination of σ_1.

Figure 3 illustrates the modelled seismicity for state A. Some events represent the response of faults, and these have double-couple mechanisms. Many events are located close to the decline and oredrives, and have crush-type mechanisms. There are also events with double-couple mechanisms scattered between the stopes and fault A. Therefore the modelling reproduces the types of events adopted in the proposed stress inversion method. The modelled seismic catalogue also includes other event types (e.g. crush-type events associated with stope abutments) which are not covered by the method and need to be excluded

from the inversion procedure by the appropriate selection of classification settings FX, FY, etc. listed in Table 1.

Table 2 Stress states used for testing

State	Azimuth/Plunge (°)			Magnitude (MPa)			R*
	σ_1	σ_2	σ_3	$\lvert\sigma_1\rvert$	$\lvert\sigma_2\rvert$	$\lvert\sigma_3\rvert$	
A	255/0	345/0	–/90	60	40	20	0.5
B	195/0	285/0	–/90	60	40	20	0.5
C	135/0	225/0	–/90	60	40	20	0.5
D	255/0	345/0	–/90	60	50	20	0.25
E	255/0	345/0	–/90	60	30	20	0.75
F	75/30	345/0	255/60	60	40	20	0.5
G	75/60	345/0	255/30	60	40	20	0.5

* Stress ratio $R = (|\sigma_1| - |\sigma_2|)/(|\sigma_1| - |\sigma_3|)$

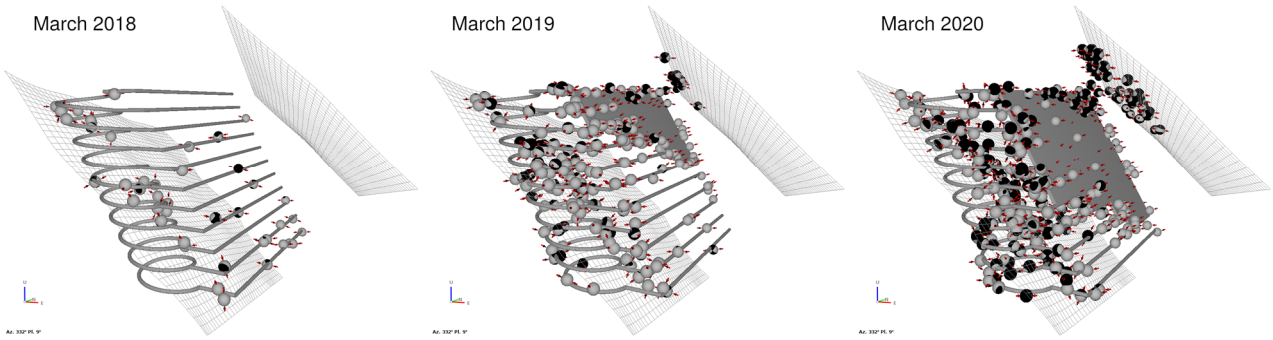

Figure 3 Modelled seismic events for stress state A. Seismic events are shown using beachballs with red dipoles indicating the P-axis orientation. Sizing is constant (i.e. does not depend on source parameters). The events are presented in a differential mode (i.e. the plot for March 2020 contains events modelled for the March 2020 mining step)

3.1 Results for reference case A

The performance of the stress inversion method is considered in detail for the reference case. The following event-classification settings listed in Table 1 were used:

- The distance between the sources of structure-related events and faults A and B is less than FX = 20 m.
- One of the nodal plane poles of structure-related events is within FY = 25° from the normal to the nearest face of faults A or B.
- The distance between stopes and the sources of structure-related and scattered events is more than FZ = SX = 30 m.
- The distance between the sources of tunnel-related events and active (existing at the time of event) tunnels is less than CX = 10 m.

Figure 4 shows the 251 events that were associated with fault surfaces and the results of stress inversion for them.

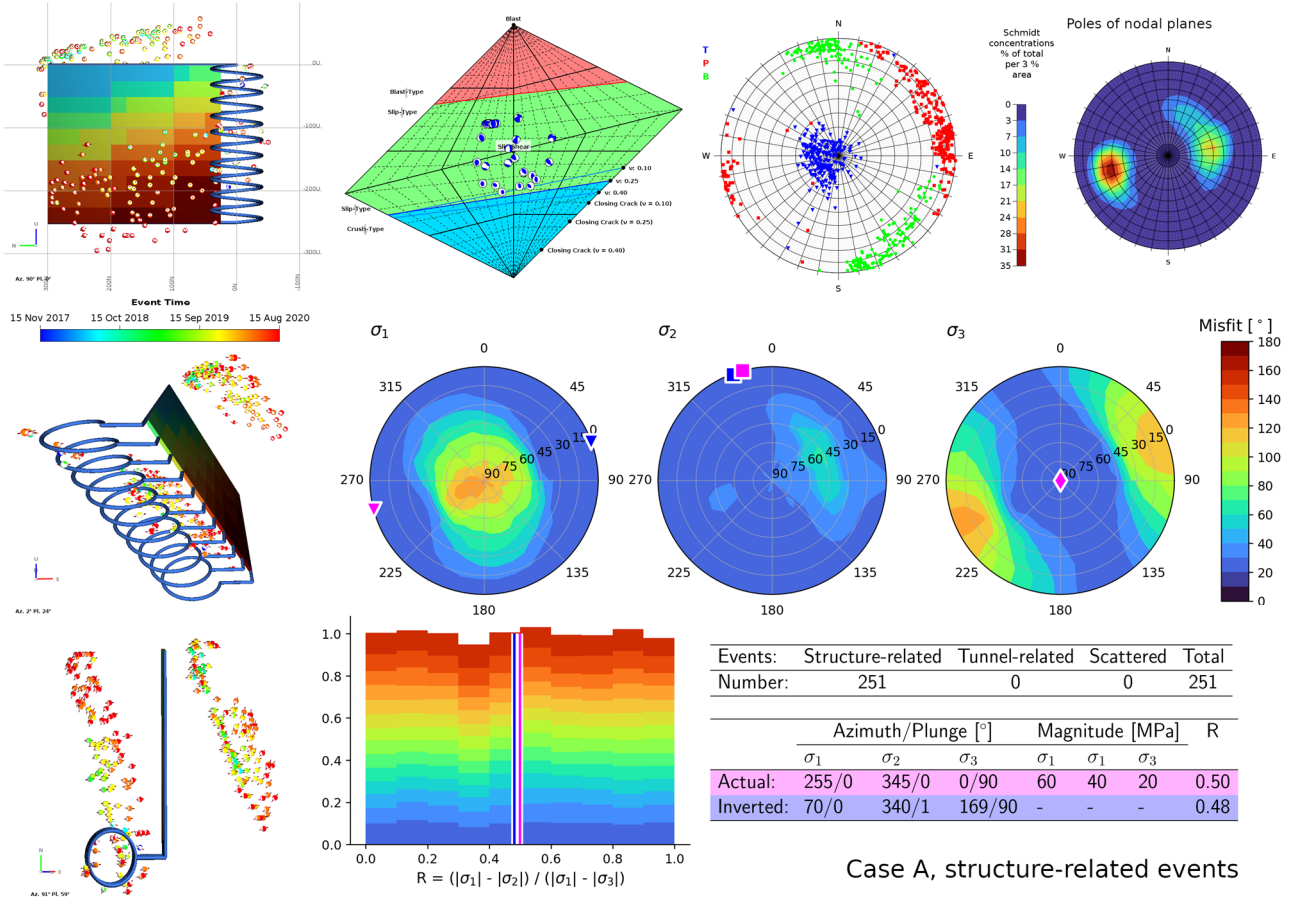

Events:	Structure-related	Tunnel-related	Scattered	Total
Number:	251	0	0	251

	Azimuth/Plunge [°]			Magnitude [MPa]			R
	σ_1	σ_2	σ_3	σ_1	σ_1	σ_3	
Actual:	255/0	345/0	0/90	60	40	20	0.50
Inverted:	70/0	340/1	169/90	-	-	-	0.48

Figure 4 Input data and results of stress inversion for structure-related events in the reference case A. The images in the left show, in section and plan views, the location of selected seismic events, which are rendered as beachballs coloured by time. Hudson source-type plot and lower-hemisphere stereonet plots in the top row summarise the moment tensors. The stereonet plots in the middle row display the misfit between seismic data and stress state for principal stresses. The superimposed magenta symbols indicate the actual stress orientations used in the modelling of seismicity, whereas the blue symbols give the inverted orientations. A histogram of misfit for the parameter R is given in the bottom row, with the actual and inverted values superimposed as magenta and blue vertical lines, respectively

- The spatial distribution of events is shown in left-hand plots. These confirm that the selected events are attributed to faults.
- The source-type plot of Hudson et al. (1989) verifies that events in the dataset are of slip-type.
- The stereonet plots show that P-axes predominantly trend sub-horizontally east-northeast, but take on a range of values: T-axes are sub-vertical; B-axes trend north-northwest; and nodal plane poles are plunging approximately 45° to east-northeast and west-southwest.
- Estimated orientations of σ_1, σ_2, and σ_3 are shown as blue markers in stereonets in the middle row, and closely match actual orientations (magenta markers).
- The R value is also accurately estimated as shown in the histogram.

Figure 5 shows tunnel-related seismicity (comprising 729 events) and stress inverted from it. The orientations of principal stresses are assessed accurately, although R is underestimated.

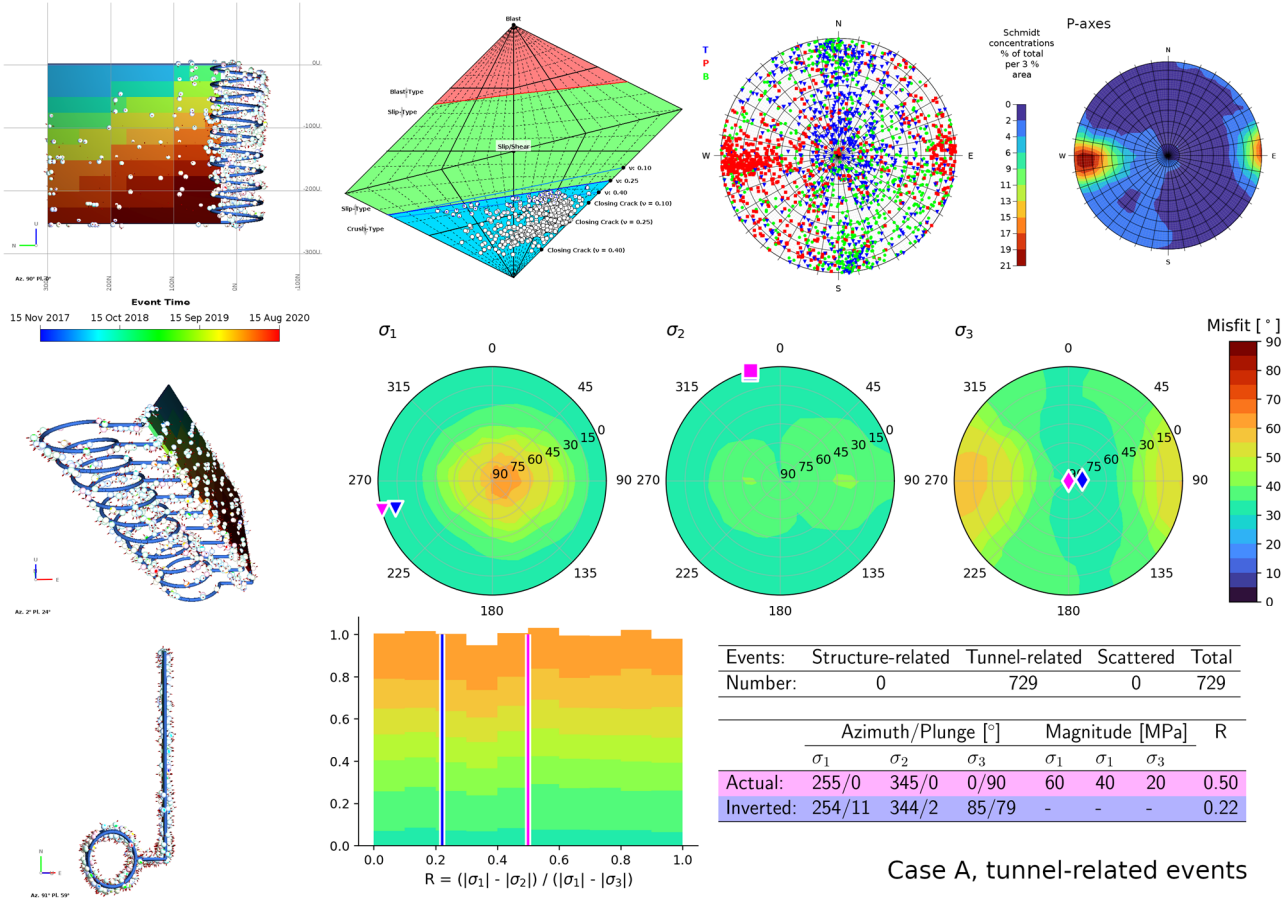

Events:	Structure-related	Tunnel-related	Scattered	Total
Number:	0	729	0	729

	Azimuth/Plunge [°]			Magnitude [MPa]			R
	σ_1	σ_2	σ_3	σ_1	σ_1	σ_3	
Actual:	255/0	345/0	0/90	60	40	20	0.50
Inverted:	254/11	344/2	85/79	-	-	-	0.22

Figure 5 Input data and results of stress inversion for tunnel-related events in reference case A

The scattered slip-type events are presented in Figure 6 (top). The inverted value of σ_3 is in very good agreement with the actual σ_3 value, whereas the other inverted principal axes are rotated 24° from the actual stresses. The stress ratio parameter is resolved correctly.

The total solution based on the combination of all three sub-sets of events is shown in Figure 6 (bottom). The directions of inverted σ_1 and σ_2 deviate from the corresponding actual directions by 14°. The difference between the inverted and actual σ_3 orientation is 6°. The R value is slightly underestimated.

Note that the final result of the proposed SIMS method (Figure 6 bottom) is based on 1,190 events, whereas conventional stress inversion methods can utilise only a small portion of this data (i.e. only the subset of scattered events, which accounts for only 18% of the combined dataset).

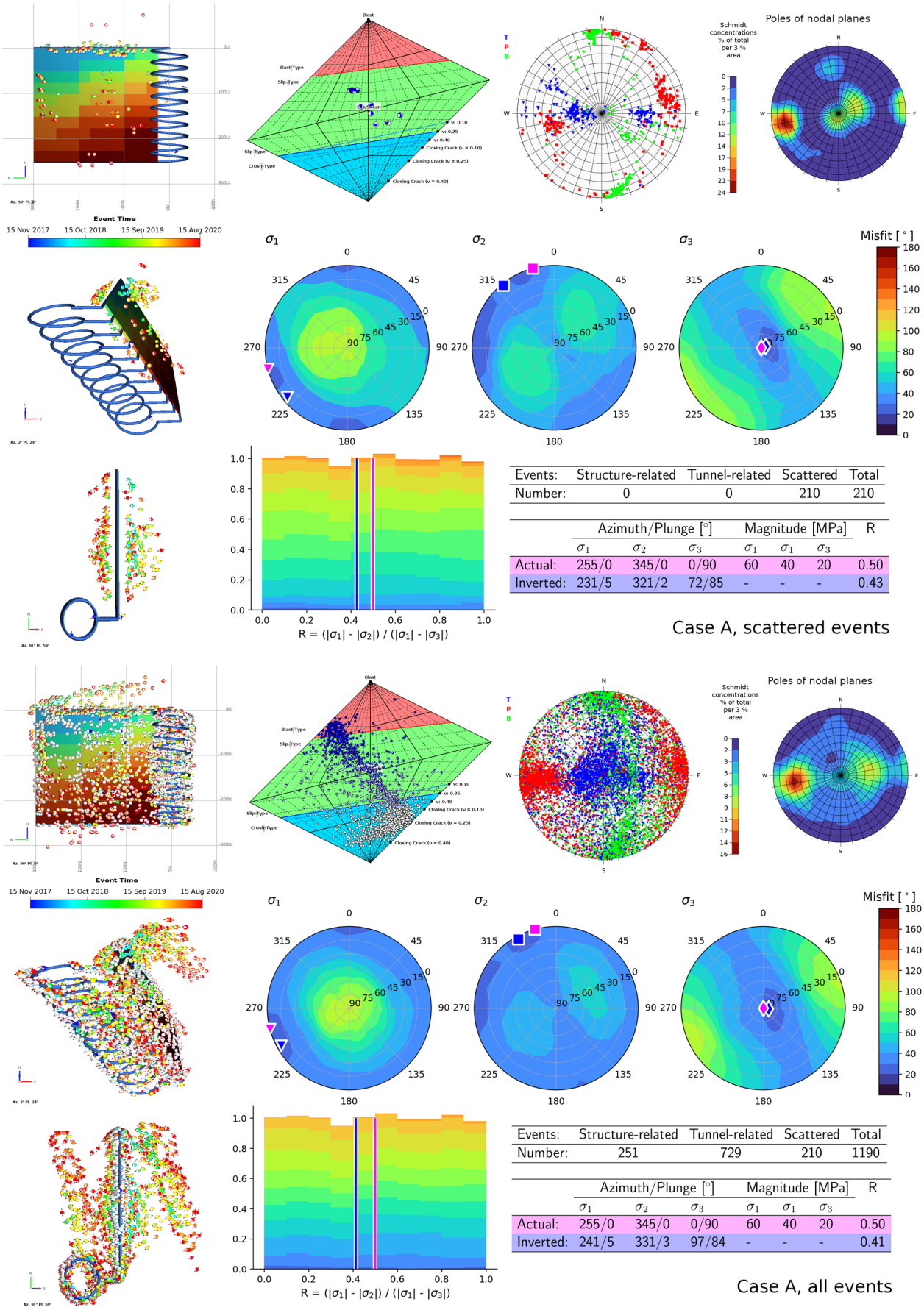

Events:	Structure-related	Tunnel-related	Scattered	Total
Number:	0	0	210	210

	Azimuth/Plunge [°]			Magnitude [MPa]			R
	σ_1	σ_2	σ_3	σ_1	σ_1	σ_3	
Actual:	255/0	345/0	0/90	60	40	20	0.50
Inverted:	231/5	321/2	72/85	-	-	-	0.43

Events:	Structure-related	Tunnel-related	Scattered	Total
Number:	251	729	210	1190

	Azimuth/Plunge [°]			Magnitude [MPa]			R
	σ_1	σ_2	σ_3	σ_1	σ_1	σ_3	
Actual:	255/0	345/0	0/90	60	40	20	0.50
Inverted:	241/5	331/3	97/84	-	-	-	0.41

Figure 6 Input data and results of stress inversion for scattered events (top) and all events (bottom) in reference case A

3.2 Results for case B

The maximum principal stress in case B is oriented approximately parallel to the orebody, which reduces the expected seismic response (in terms of all event types). The number of events usable for stress inversion is approximately half that of case A. Figure 7 (top) shows that the inverted orientations of principal stresses are within 15° of the actual principal stresses. The stress ratio parameter R is resolved correctly.

3.3 Results for case C

The maximum principal stress in case C is trending in a northwest-southeast direction, which makes faults A and B less prone to slip. Consequently the number of structure-related events is small. The response in terms of tunnel-related and scattered events is significant. Figure 7 (middle) shows that the inversion of principal stress orientations is accurate. The stress ratio parameter R is overestimated.

3.4 Results for case D

The orientation of principal stresses in case D is the same as in reference case A, but the magnitude of σ_2 is closer to σ_1 than to σ_3 (i.e. near a state of uniaxial unloading). This explains the poor resolution of the orientations of σ_1 and σ_2 in the inversion, as shown in Figure 7 (bottom).

3.5 Results for case E

Case E is similar to the previous case except that the magnitude of σ_2 is closer to σ_3 than to σ_1 (i.e. near a uniaxial unloading state). The inverted orientations of principal axes are within 10° from the actual directions as presented in Figure 8 (top). The histogram of the parameter R has two maxima and the inverted solution is assigned to the left one (R = 0.5), which is different from the actual value. The second/right maximum matches the actual value better.

3.6 Results for case F

Case F explores the deviation of maximum principal stress from a horizontal plane. The obtained solution most accurately replicates the actual stress state among all the considered cases (Figure 8, middle).

3.7 Results for case G

Case G has maximum principal stress plunging subparallel to the orebody. This explains why the modelled seismic response is the weakest among all the cases, however, the ‘recorded’ events are sufficient to provide reasonably accurate reconstruction of the actual stress (Figure 8, bottom).

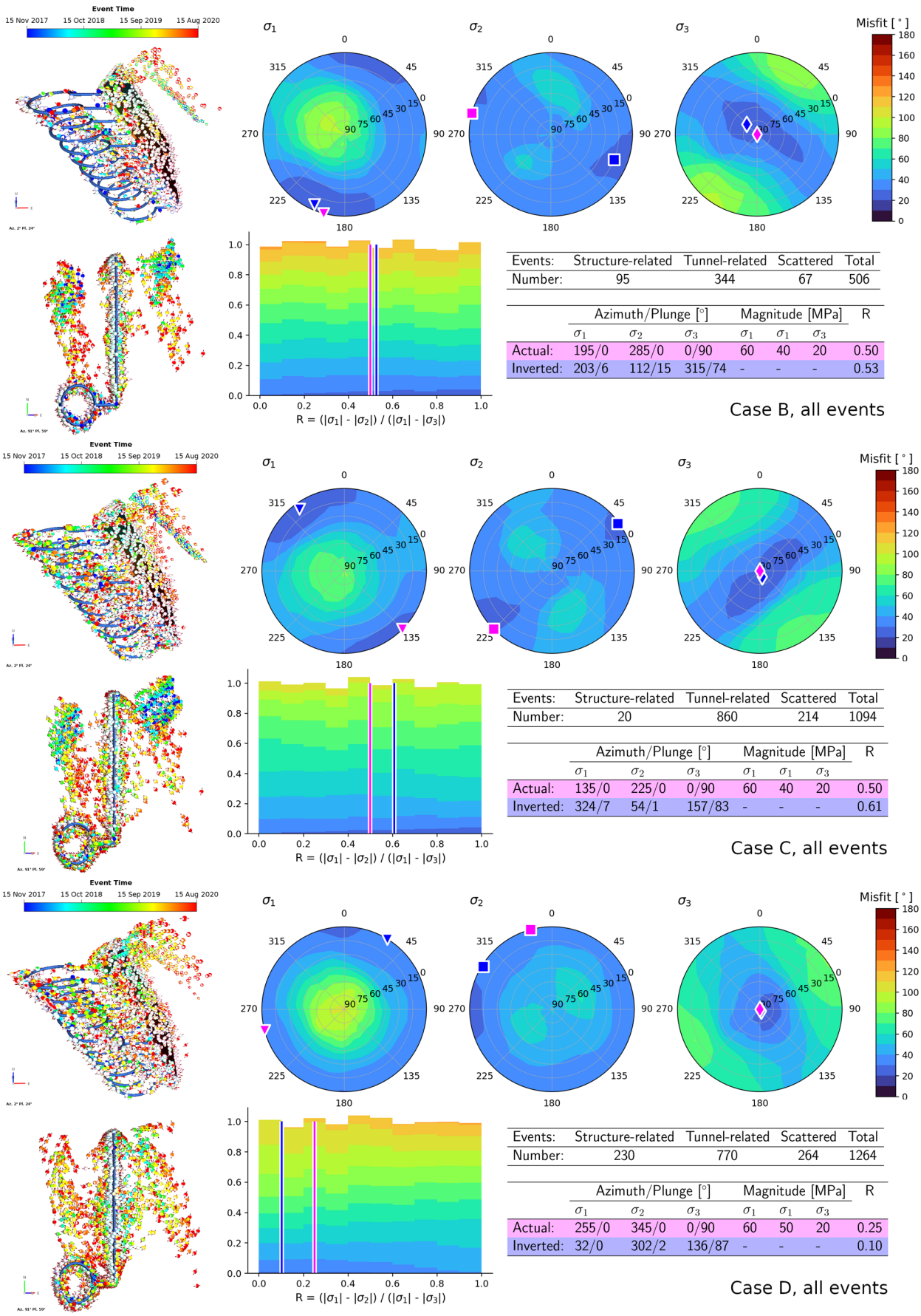

Figure 7 Input data and results of stress inversion for all events in cases B (top), C (middle) and D (bottom)

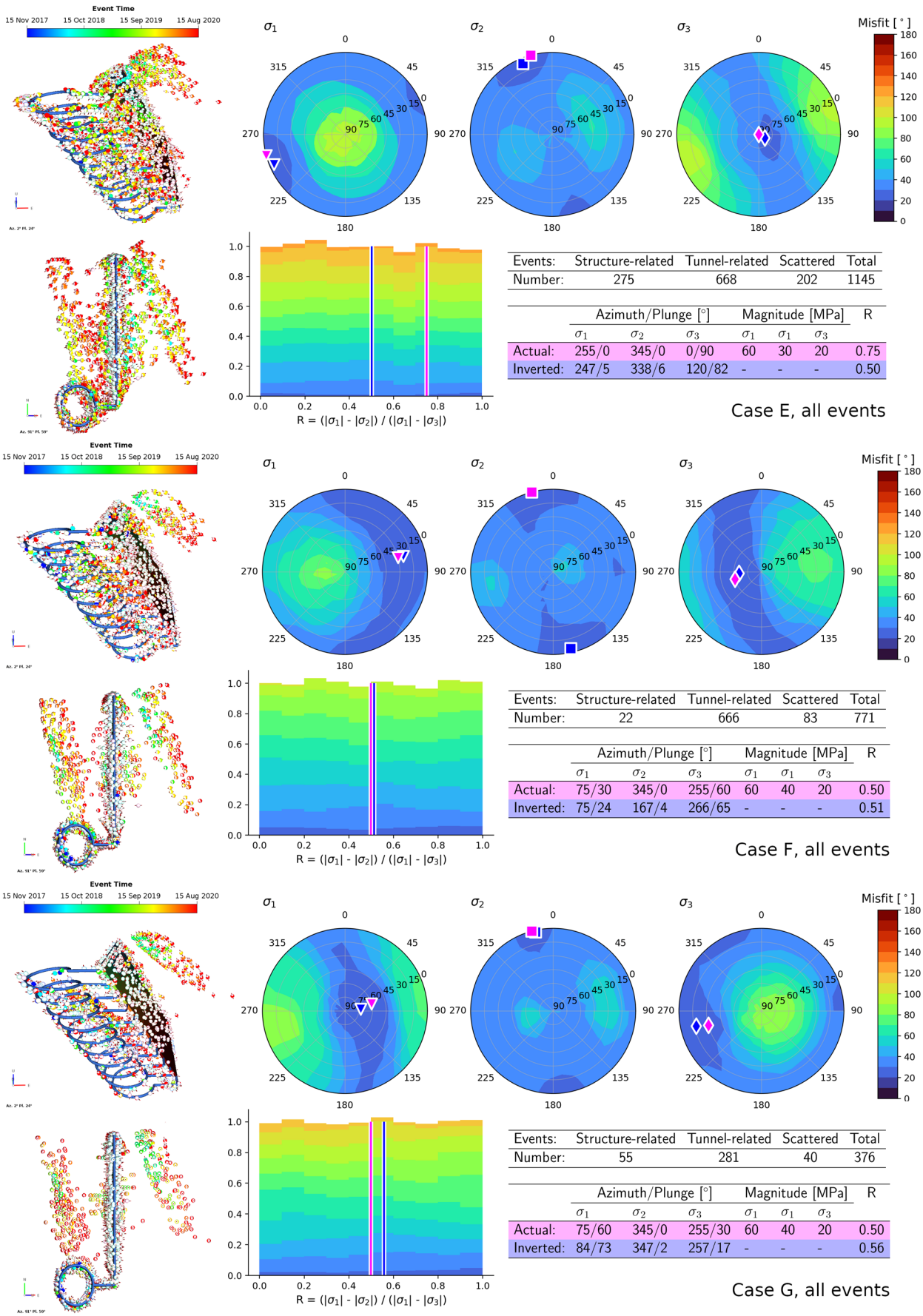

Figure 8 Input data and results of stress inversion for all events in cases E (top), F (middle) and G (bottom)

4 Application to real data

The stress measurements conducted at a block caving mine were presented by Malovichko (2022). The measurements were compared with inversion results obtained using the linear stress inversion with bootstrapping (LSIB) method (Michael 1984, 1987; Hardebeck & Hauksson 2001). The inversion was based on 53 slip-type scattered seismic events which satisfy the requirements of the method described in Section 1.

To test the proposed SIMS method, the analysed dataset was extended by including slip-type events associated with known structures and crush-type events attributed to tunnels and raisebores. The location accuracy is sufficiently good to adopt the same event-classification settings as were used for synthetic data in Section 3. The results of inversion are summarised in Figure 9 and in the last row of Table 3. The results of the LSIB inversion from Malovichko (2022) are shown for reference. Note that the new method used 122 events, with scattered events comprising less than half of these.

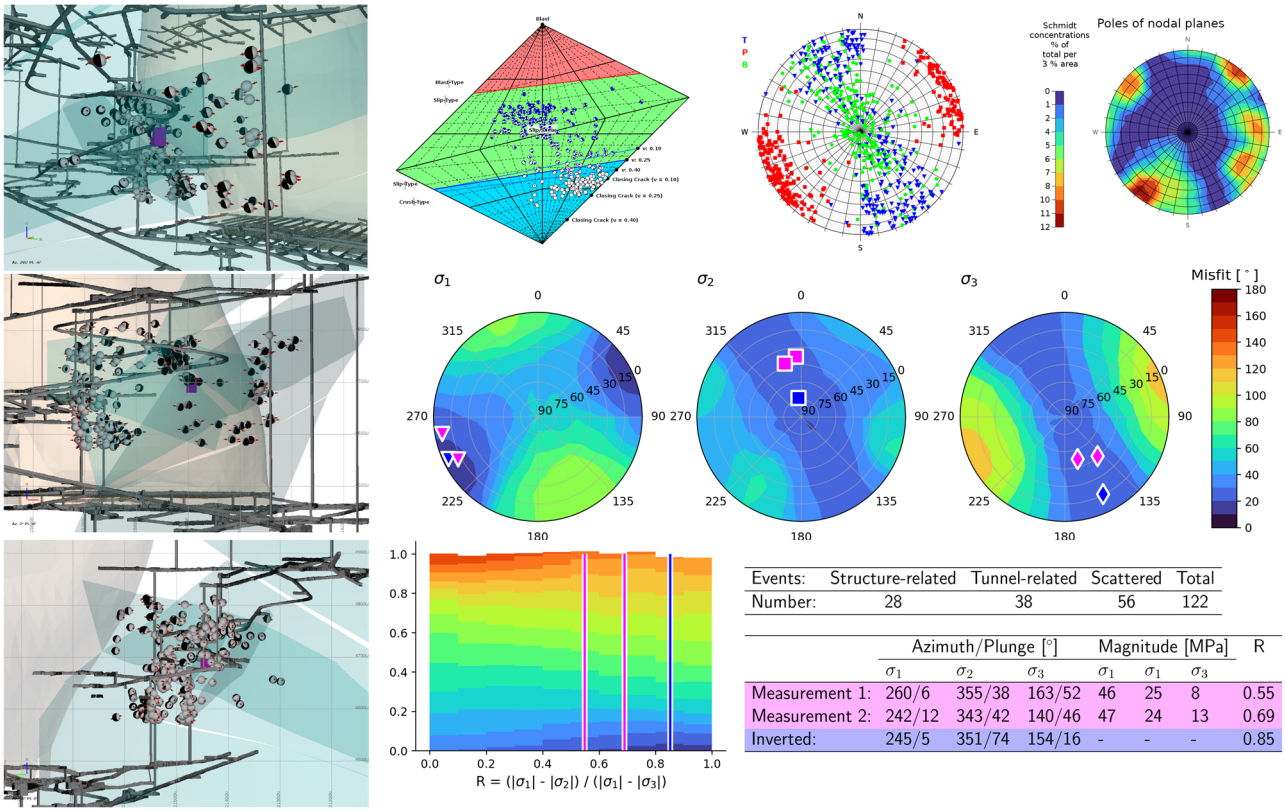

Figure 9 Input data and results of stress inversion for a real case. The locations of stress measurements are shown in plots on the left using magenta boxes

Table 3 Comparing stress measurements with stress inversion results for a real mine

Type	Azimuth/plunge (°)			Magnitude (MPa)			R
	σ_1	σ_2	σ_3	$\lvert\sigma_1\rvert$	$\lvert\sigma_2\rvert$	$\lvert\sigma_3\rvert$	
Measurement 1	260/6	355/38	163/52	46.3	25.2	7.9	0.55
Measurement 2	242/12	343/42	140/46	47.3	23.5	12.8	0.69
LSIB inversion	253/4	108/86	344/2	–	–	–	0.78
SIMS inversion	245/5	351/74	154/16	–	–	–	0.85

The inverted stress state is in good agreement with the measurements in terms of the direction of maximum principal stress, σ_1. The agreement is poorer for the directions of intermediate, σ_2, and minor,

σ_3, principal stresses. The difference between the measured and inverted orientations of these stresses is approximately 20°.

The inverted stress ratio parameter, R, suggests that the magnitudes of σ_2 and σ_3 are actually closer to each other, compared to the measurements. However the measurements themselves show substantial variance in the parameter R (0.55 for measurement 1 versus 0.69 for measurement 2), as might be expected considering the possible inaccuracies.

5 Conclusion

A simple method to assess the parameters of the stress field at mines using seismic source mechanisms has been proposed. The method extends the conventional stress inversion approaches applicable for focal mechanisms of tectonic earthquakes in regard to two aspects:

1. It involves a specific type of events observed at mines (events with crush-type mechanisms attributed to tunnels).
2. It utilises information available at mines (structural models and mine plans).

Similarly to conventional approaches, the inverted parameters are the orientation of principal stresses and the ratio of their magnitudes.

The method was applied to synthetic seismicity (modelled for various prescribed in situ stresses) and to real mining-induced seismicity recorded around the locations of stress measurements. The application demonstrated that the obtained solutions are reasonably accurate in terms of the recovery of principal stress orientations (the error is of the order of 10 to 20°).

The method is suitable for typical mine-wide seismic observations for which seismic source mechanisms characterise episodes of sudden inelastic deformation and driving stress within rock mass volumes having dimensions in the order of tens or hundreds of metres. If the scale of seismic monitoring is much smaller (e.g. high-resolution observations of an individual tunnel using a local array of accelerometers) then the method needs to be adjusted (i.e. local heterogeneity of the stress field may need to be taken into account and the adopted interpretation of crush-type mechanisms may not be applicable).

Conventional stress inversion methods (e.g. FMSI and LSIB) provide not only the optimal solution but also its uncertainty, as discussed in detail by Hardebeck & Hauksson (2001). The proposed SIMS method makes it possible to characterise the uncertainty only qualitatively in the form of plots of misfit angle (stereonets and historgram). Proper quantification of uncertainty is desirable and this limitation of the method needs to be addressed in future.

There are several other directions of future work:

- The SIMS method described in this paper is based on geometrical relations between the deformation within the seismic sources and the driving stress, i.e. the misfit is quantified in terms of angular difference and it does not depend on the stress magnitudes. It is reasonable to extend the approach towards utilisation of the magnitudes of driving stresses (e.g. to take into account the magnitudes of shear traction and normal stress for nodal planes of scattered events and for slip surfaces of fault-related events, or the magnitude of maximum in-plane stress for crush-type events associated with tunnels).
- The SIMS method adopts a binary classification of events (slip-type versus crush-type). There are intermediate types of events which correspond to shear/slip in the proximity of an excavation. A mathematical framework making it possible to recover the ingredients of these two constituting processes from seismic source mechanisms was suggested by Rigby (2023) and Rigby et al. (2024). This framework may help to include non-crush-type events associated with tunnels and tabular orebodies into the stress inversion method.

Acknowledgement

The authors appreciate the permission of mine management to present real data, and thank the reviewers for their constructive and helpful comments.

References

Abolfazlzadeh, Y & McKinnon, SD 2017, 'Stress field characterisation in Nickel Rim South Mine using seismic stress inversion', in J Wesseloo (ed.), *Deep Mining 2017: Proceedings of the Eighth International Conference on Deep and High Stress Mining*, Australian Centre for Geomechanics, Perth, pp. 247–256, https://doi.org/10.36487/ACG_rep/1704_16_Abolfazlzadeh

Angelier, J 1984, 'Tectonic analysis of fault slip data sets', *Journal of Geophysical Research*, vol. 89, pp. 5835–5848.

Basson, G, Bassom, AP & Salmon, B 2021, 'Simulating mining-induced seismicity using the material point method', *Rock Mechanics and Rock Engineering*, vol. 54, no. 9, pp. 4483–4503.

Brzovic, A, Skarmeta, J, Blanco, B, Dunlop, R & Sepuvelda, MP 2017, 'Sub-horizontal faulting mechanism for large rockbursts at the El Teniente mine', in Vallejos, J.A. (ed), *Proceedings of the 9th International Symposium on Rockbursts and Seismicity in Mines*, pp. 124–132.

Gephart, JW 1990, 'FMSI: A FORTRAN program for inverting fault/slikenside and earthquake focal mechanism data to obtain the regional stress tensor', *Computers and Geosciences*, vol. 16, pp. 953–989.

Gephart, JW & Forsyth, DW 1984, 'An improved method for determining the regional stress tensor using earthquake focal mechanism data: application to the San Fernando earthquake sequence', *Journal of Geophysical Research*, vol. 89, pp. 9305–9320.

Hardebeck, JL & Hauksson, E 2001, 'Stress orientations obtained from earthquake focal mechanisms: What are appropriate uncertainty estimates?', *Bulletin of the Seismological Society of America*, vol. 91, no. 2, pp. 250–262.

Harmsen, SC & Rogers, AM 1986, 'Inferences about the local stress field from focal mechanisms: applications to earthquakes in the southern Great Basin of Nevada', *Bulletin of the Seismological Society of America*, vol. 76, pp. 1560–1572.

Hudson, JA, Pearce, RG & Rogers, RM 1989, 'Source type plot for inversion of the moment tensor', *Journal of Geophysical Research*, vol. 94, no. B1, pp. 765–774.

Kagan, YY 1991, '3-D rotation of double-couple earthquake sources', *Geophysical Journal International*, vol. 106, pp. 709–716.

Malovichko, D 2020, 'Description of seismic sources in underground mines: theory', *Bulletin of the Seismological Society of America*, vol. 110, pp. 2124–2137.

Malovichko, D 2022, 'Keynote: utility of seismic source mechanisms in mining', in M Diederichs (ed.), *Proceedings of the 10th International Symposium on Rockbursts and Seismicity in Mines*.

Malovichko, D & Rigby, A 2022, 'Description of seismic sources in underground mines: Dynamic stress fracturing around tunnels and strainbursting', *arXiv*, https://doi.org/10.48550/arXiv.2205.07379.

Michael, AJ 1984, 'Determination of stress from slip data: faults and folds', *Journal of Geophysical Research*, vol. 89, pp. 11517–11526.

Michael, AJ 1987, 'Use of focal mechanisms to determine stress: a control study', *Journal of Geophysical Research*, vol. 92, pp. 357–368.

McKenzie, DP 1969, 'The relation between fault plane solutions for earthquakes and the directions of the principal stresses', *Bulletin of the Seismological Society of America*, vol. 59, no. 2, pp. 591–601.

Nairn, JA 2003, 'Material point method calculations with explicit cracks', *Computer Modeling in Engineering and Sciences*, vol. 4, no. 6, pp. 649–664.

Rigby, A 2022, 'Numerical modelling of the T20 chamber', *Technical Report*, Institute of Mine Seismology, CAD-REP-T20MODELLING-20220504-ARv1.

Rigby, A 2023, 'Physically motivated moment-tensor decomposition for mining-induced seismicity', *Geophysical Journal International*, vol. 236, iss. 1, pp. 443–455.

Rigby, A, Malovichko, D & Gerber, J 2024, 'A seismic source model for strainbursting of tabular stopes', *Journal of South African Mining and Metallurgy* (submitted).

Ryder, JA 1988, 'Excess shear stress in the assessment of geologically hazardous situations', *Journal of South African Mining and Metallurgy*, vol. 88, no. 1, pp. 27–39.

Trifu, C-I & Shumila, V 2011, 'The analysis of stress tensor determined from seismic moment tensor solutions at Goldex Mine Quebec', *Proceedings of the 45th US Rock Mechanics Symposium*, paper 11-584, American Rock Mechanics Association, Alexandria.

Urbancic, TI, Trifu, C-I & Young, RP 1993, 'Microseismicity derived fault-planes and their relationship to focal mechanism, stress inversion, and geologic data', *Geophysical Research Letters*, vol. 20, no. 22, pp. 2475–2478.